HHS Public Access

Author manuscript

Virology. Author manuscript; available in PMC 2020 June 01.

Published in final edited form as:

Virology. 2019 September ; 535: 232–240. doi:10.1016/j.virol.2019.07.012.

Identification of key hemagglutinin residues responsible for cleavage, acid stability, and virulence of fifth-wave highly pathogenic avian influenza A(H7N9) viruses

Xiangjie Sun[a], **Jessica A. Belser**[a], **Hua Yang**[a], **Joanna A. Pulit-Penaloza**[a], **Claudia Pappas**[a], **Nicole Brock**[b], **Hui Zeng**[a], **Hannah M. Creager**[a], **James Stevens**[a], **Taronna R. Maines**[a,*]

[a]Influenza Division, National Center for Immunization and Respiratory Diseases, Centers for Disease Control and Prevention, Atlanta, GA, USA

[b]CNI Advantage LLC, Norman, OK, USA

Abstract

We previously demonstrated that despite no airborne transmissibility increase compared to low pathogenic avian influenza viruses, select human isolates of highly pathogenic avian influenza A(H7N9) virus exhibit greater virulence in animal models and a lower threshold pH for fusion. In the current study, we utilized both *in vitro* and *in vivo* approaches to identify key residues responsible for hemagglutinin (HA) intracellular cleavage, acid stability, and virulence in mice. We found that the four amino acid insertion (-KRTA-) at the HA cleavage site of A/Taiwan/1/2017 virus is essential for HA intracellular cleavage and contributes to disease in mice. Furthermore, a lysine to glutamic acid mutation at position HA2-64 increased the threshold pH for HA activation, reduced virus stability, and replication in mice. Identification of a key residue responsible for enhanced acid stability of A(H7N9) viruses is of great significance for future surveillance activities and improvements in vaccine stability.

Keywords

Influenza virus; A(H7N9); Hemagglutinin cleavage; Fusion; Acid stability; Virulence; Mice

1. Introduction

Influenza A virus (IAV) is an enveloped virus with a negative sense, single-stranded, segmented RNA genome (Fields et al., 2007). The two major surface glycoproteins embedded into the viral membrane are hemagglutinin (HA) and neuraminidase (NA), and represent the major antigenic proteins of the virus. Based on the antigenic properties of the HA and NA proteins, influenza viruses have been classified into 18 HA (H1–H18) and 11 NA (N1–N11) subtypes (Tong et al., 2013). The HA and NA proteins also play important biological functions in the virus life cycle; the HA binds to sialic acid receptors and

*Corresponding author. tmaines@cdc.gov (T.R. Maines).

Appendix A.: Supplementary data

Supplementary data to this article can be found online at https://doi.org/10.1016/j.virol.2019.07.012.

mediates virus entry and fusion between viral and host endosomal membranes, and the NA cleaves sialic acid residues to release progeny viruses from host cells (Fields et al., 2007). IAV has a wide host range in both avian and mammalian species, including humans (Fields et al., 2007). Although interspecies transmission of influenza viruses between avian and human hosts is rare, certain subtypes, predominantly H5 and H7 subtype viruses, have demonstrated the ability to occasionally cross the species barrier and cause sporadic human infections or even death, highlighting the threat to public health posed by such viruses (Short et al., 2015).

In May 2013, a novel reassortant low pathogenic avian influenza (LPAI) A(H7N9) virus emerged in China, resulting in the first cases of documented human infection with an A(H7N9) virus (Gao et al., 2013). Since then, LPAI A(H7N9) virus continued to spread throughout China, and has caused six complete epidemic waves of human infection (CDC, 2018). As of February 2019, the Food and Agriculture Organization of the United Nations (FAO) has reported over 1,560 laboratory-confirmed human infections including more than 600 deaths (FAO, 2019). In early 2017, antigenically divergent highly pathogenic avian influenza (HPAI) A(H7N9) viruses were isolated for the first time from humans, with concurrent detection of genetically similar viruses in poultry and environmental samples (Zhang et al., 2017; Ke et al., 2017; Zhou et al., 2017; Yang et al., 2017). The virulence of avian influenza virus in chickens is largely determined by the cleavability of the HA precursor protein HA0 (Short et al., 2015). LPAI viruses possess a single arginine residue at the HA cleavage site that is cleaved by localized extracellular proteases, often causing only mild or asymptomatic infections; in contrast, HPAI viruses typically contain multiple basic residues at the HA cleavage site that can be cleaved by ubiquitous, intracellular subtilisin-like serine proteases, causing systemic infections with high mortality in chickens (Short et al., 2015). Compared to LPAI A(H7N9) virus, HPAI A(H7N9) viruses have acquired a 4-amino acid (aa) insertion (-K-R-T/A-A/K-) at the conserved HA cleavage site, shown to be essential for high virulence in chickens (Qi et al., 2018). However, the relative contribution of the HPAI A(H7N9) virus polybasic cleavage site to viral pathogenicity in mammalian hosts has yet to be determined.

Following the initial LPAI A(H7N9) outbreak in China, substantial efforts have been made to understand the molecular mechanisms of A(H7N9) virus cross-species transmission and to assess its pandemic risk to humans. Compared to most avian influenza viruses, which exclusively bind to α-2,3-linked sialic acid (avian-like) receptors, LPAI A(H7N9) isolates have exhibited a certain binding capacity for α-2,6-linked sialic acid (human-like) receptors in addition to a predominant binding preference for avian-like receptors (Xiong et al., 2013; Yang et al., 2018). Furthermore, most human LPAI A(H7N9) isolates possess substitutions in polymerase proteins such as PB2-E627K, indicative of enhanced viral replication in mammals (Hatta et al., 2001). Select LPAI A(H7N9) isolates are capable of limited transmission via respiratory droplets in the ferret model, a property not shared by most avian influenza viruses (Richard et al., 2013; Watanabe et al., 2013; Belser et al., 2013). Both the receptor binding capacity for human-like receptors, and the presence of mammalian host adaptation mutations in the polymerase proteins, is thought to contribute to LPAI A(H7N9) virus interspecies transmission and improved adaptation to mammals (Watanabe et al., 2014).

We recently demonstrated that despite no airborne transmissibility increase compared to LPAI A(H7N9) viruses, select HPAI A(H7N9) human isolates possess heightened mammalian virulence with an extended tissue tropism in animal models and a lowered threshold pH for membrane fusion, a trait potentially associated with enhanced transmission in mammals (Sun et al., 2018). However, a comprehensive understanding of the biological properties associated with HPAI A(H7N9) virulence and mammalian transmission has yet to be identified. In this study, we focused on the HA protein of HPAI A(H7N9) viruses and used both *in vivo* and *in vitro* approaches combined with sequence and structural analyses to identify key residues responsible for HA cleavage, acid stability, and virulence in mammalian hosts. The results from our study will ultimately help us better understand how A(H7N9) influenza viruses evolve and adapt to mammalian hosts, and improve surveillance efforts to quickly identify circulating zoonotic influenza viruses with an increased capacity for human infection and the potential to cause a pandemic.

2. Results

Comparison of fifth-wave HPAI and LPAI A(H7N9) virus HA proteins.

During the fifth epidemic wave (October 1, 2016–September 30, 2017) in China, a total of 858 A(H7N9) HA sequences, derived from 733 LPAI and 125 HPAI isolates or passages of isolates (as of November 2018), were deposited in the Global Initiative on Sharing All Influenza Data (GISAID) database. The most striking difference between the LPAI and HPAI A(H7N9) viruses is a characteristic 4-aa insertion (-KRTA-, P5–P2 position) adjacent to the conserved arginine (R) residue at the HA cleavage site (HA0 cleaves between R/G) of HPAI viruses. This results in a consensus sequence of (-K-R-T-A-R/G-). which meets the minimum requirement for a furin protease cleavage motif (-R/K-X-X-R) (Fig. 1). Beyond differences at the HA cleavage site, the consensus HA sequence of HPAI A(H7N9) viruses has seven aa substitutions including I38T, T112P, K164E, L217Q, I317V, G320R (H7 numbering) in the HA1, and E64K in the HA2, compared to that of LPAI A(H7N9) viruses (Fig. 1). Interestingly, the substitution at G320R is more prevalent among HPAI A(H7N9) human isolates (55/56) compared to avian or environmental isolates, which favor glycine (G) (37/69) at this position (Fig. 1). The presence of R at position 320 adds an additional basic residue at the HA cleavage site and generates a stretch of 4 basic residues of (-K-R$_{320}$-K-R-T-A-R/G. underlined and correspond to P7-P4 positions), which would potentially enhance the cleavage efficiency mediated by furin-like proteases (Shiryaev et al., 2013). In conclusion, our sequence analysis of fifth-wave A(H7N9) viruses shows that HPAI A(H7N9) viruses have evolved to acquire novel substitutions in the HA gene, which may potentially contribute to HA cleavability, antigenicity, and virulence.

HA residues contribute to the cleavage and the threshold pH for HA activation

The presence of a 4-aa insertion (-K-R-T-A-) in the HA of HPAI A(H7N9) viruses generates a sequence at the HA cleavage site for intracellular furin-like serine protease recognition (Thomas, 2002). To confirm whether the HPAI A(H7N9) HA can be cleaved by intracellular proteases, we expressed the HA proteins from HPAI A/Taiwan/1/2017 (TW/17) or LPAI A/Anhui/1/2013 (AH/13) viruses by plasmid transfection in 293T cells and evaluated HA cleavage by Western blot using anti-HA antibody. It has been previously demonstrated that

some HAs of HPAI viruses, which can undergo conformational changes at high pH values (> 5.5), require M2 ion channel protein activity in the trans-Golgi compartment to prevent the cleaved HA from being inactivated and degraded during its transport through secretory pathways (Takeuchi and Lamb, 1994; Alvarado-Facundo et al., 2015). Therefore, in our study, the plasmid encoding the M gene of A/Puerto Rico/8/1934 (PR8) virus was co-transfected with TW/17 virus HA at a 1:4 ratio to stabilize the native form of HA. We found that the mature, surfaced-expressed TW/17 virus HAs, but not AH/13 virus HAs, can be cleaved into HA1, HA2 in the absence of extracellular proteases (Fig. 2). To further investigate whether the 4-aa insertion, or any other substitutions, in the HPAI A(H7N9) HA contribute to the HA intracellular cleavage, we generated seven single aa mutations (T38I, P112T, E164K, Q217L, V317I, R320G in HA1 and K64E in HA2) or the 4-aa insertion deletion mutant (Del 321–324) in the TW/17 virus HA to mimic the consensus sequence of LPAI A(H7N9) viruses, and then assessed their cleavage in 293T cells. As shown in Fig. 2A, none of the single mutants, including R320G, affected HA intracellular cleavage, but in contrast, the removal of the HA insertion (-KRTA-) abolished HA cleavage based on the absence of the HA1 and HA2, the cleaved products of HA0.

We have previously reported that select fifth-wave HPAI and LPAI A(H7N9) viruses have a threshold pH of HA activation of 5.4 and 5.7–5.8, respectively (Sun et al., 2018; Belser et al., 2016). Both HA and NA genes have been shown to modulate the pH for membrane fusion (Russell et al., 2018). To identify the main determinant for the differing pH thresholds exhibited by HPAI and LPAI A(H7N9) viruses, we expressed the HA protein from either HPAI TW/17 or LPAI AH/13 virus by plasmid transfection in Vero cells and compared the pH threshold of HA activation via a syncytia formation assay. We found that expression of the TW/17 or AH/13 virus HA protein alone exhibited an HA activation pH threshold of 5.4 or 5.8, respectively (Fig. 2B), consistent with results using wild-type, infectious virus, which confirms that the HA protein is the main determinant in modulating the fusion pH for A(H7N9) viruses. Next, we used the same approach to compare the fusion activation pH of the HA proteins of either wild-type or mutant forms (inclusive of the seven aforementioned single aa substitutions and the 4-aa deletion) and found that none of the mutations, except HA2-K64E, caused a shift in the pH of HA activation. The HA2-K64E mutant HA increased the threshold pH of HA activation from 5.4 to 5.8 (Fig. 2B), indicating that HA2-K64 is a key residue in the HA protein, which controls the pH at which HA activation occurs for this HPAI A(H7N9) virus. Taken together, we conclude that the 4 aa-insertion confers intracellular cleavability of the HA, and the residue HA2-K64 modulates the threshold pH for HPAI A(H7N9) HA proteins.

Structural modeling of HA2-K64 in the HPAI A(H7N9) HA protein.

To gain better insight into how HA2-K64 is involved in modulating the threshold pH of HA activation, the positions of seven amino acids in the TW/17 virus, which are unique for HPAI H7N9 viruses, were located using the HA model from the HPAI A(H7N9) A/Guangdong/17SF003/2016 (PDB ID: 6D7U) virus. HA1 amino acids T38 and PI 12 are near the antigenic sites C and A, respectively, whereas Q217 is located at the receptor binding site and E164 is a surface residue in the head region (Fig. 3). Although V317 and R320 are located in the fusion peptide region, they are not visible in the model. K64 in HA2 is located

in the B-loop region, which, upon exposure to acid, undergoes a conformational change to become part of the long helix, and is predicted to form hydrogen bonds with the conserved HA2-N79 and the glycans at HA2-N82 from the neighboring monomer. The change from lysine (K) to glutamic acid (E) not only alters the surface charge in this area, but also potentially decreases the local stability by weakening the interaction with HA2-N79 and the glycan at HA2-N82. Our HA structural analysis provides further evidence that the HA2-K64 residue plays an important role in maintaining HA structural stability and is capable of modulating the pH requirement for HA activation.

Replication kinetics and fusion activity of wild-type or mutant recombinant PR8:TW/17-HA/NA viruses.

Our initial *in vitro* assays identified key residues responsible for HA intracellular cleavage and the reduced threshold pH for HA activation in the HPAI A(H7N9) TW/17 virus HA. To better understand the role they play in viral replication, stability, and pathogenesis, we constructed recombinant influenza viruses with all internal genes from PR8 virus and the surface HA and NA genes from TW/17 virus. Wild-type, PR8:TW/17-HA/NA, and mutant viruses, PR8:TW/17-(HA1-Del321-324/R320G)/NA and PR8:TW/17-(HA2-K64E)/NA, were generated to mimic the cleavage site and the aa affecting HA activation of LPAI A(H7N9) virus, respectively. Additionally, HA1-R320G, a substitution showing predominance in avian HPAI A(H7N9) isolates, was also constructed to evaluate whether this mutation is involved in viral virulence *in vivo*, although this mutant has no effect on HA intracellular cleavage *in vitro.* The recombinant PR8 viruses bearing the wild-type or mutant HAs were first evaluated for their replicative ability in the human airway epithelial cell line Calu-3, which has been shown to express extracellular proteases that cleave the HAs of various subtypes of influenza viruses (Bottcher-Friebertshauser et al., 2011). As shown in Fig. 4A, when Calu-3 cells were inoculated at an MOI of 0.01 EID_{50}, all three mutant viruses replicated efficiently, reaching peak titers (ranging from $10^{7.8}$-$10^{8.6}$ EID_{50}/ml) by 72–96 h post inoculation (p.i.). Mutant virus, PR8:TW/17-(HA1-Del321-324/R320G)/NA, had a lower peak titer compared to the control wild-type virus ($p < 0.05$ at 72 and 96 h p.i.). Our findings suggest that having an insertion at the HA cleavage site confers a higher replication capacity in Calu-3 cells, while viruses bearing a single substitution at HA2-K64E or the absence of a basic residue at position P6 (HA1-R320G) are not significantly attenuated compared with the wild-type virus. We next compared the replication kinetics of wild-type and mutant PR8 recombinant viruses in MDCK cells, which do not express extracellular proteases for HA cleavage. Compared with the wild-type virus, the mutant virus, PR8:TW-(HA1-Del321-324/R320G)/NA, failed to replicate efficiently and reached a peak titer of only $10^{2.5}$ EID_{50}/ml at 24 h p.i. ($p < 0.0001$) in MDCK cells. However, the single aa mutant viruses (HA1-R320G or HA2-K64E) maintained comparable replication capacity at both 48 and 72 h p.i., despite reduced titers of the HA1-R320G mutant virus at an early time point (24 h, $p < 0.001$) (Fig. 4B).

To determine the effects of the mutations on the threshold pH for fusion, we inoculated Vero cell cultures with the same set of wild-type or mutant viruses and induced syncytia formation. Our results show that the virus bearing the HA2-K64E mutation possessed a threshold pH of 5.8, while the remaining three recombinant viruses maintained a fusion

threshold pH of 5.4, consistent with the wild-type PR8:TW/17-HA/NA virus (Fig. 5). Together, we conclude that the 4 amino acid insertion at HA1 ($_{321}$-KRTA-$_{324}$) contributes to virus replication and has an essential role when exogenous proteases are absent, and HA2-K64 is responsible for the reduced threshold pH for fusion activation. Both of these characteristics may also have a potential effect on virus replication *in vivo.*

Recombinant PR8:TW/17-(HA2-K64E)/NA mutant virus exhibited higher replication capacity in Vero cells and reduced stability.

The difference in the threshold pH of HA activation between PR8:TW/17-HA/NA virus with and without the HA2-K64E mutation prompted us to further compare the biological properties of these two viruses. First, we examined viral replication kinetics in Vero cells, which have been reported to have a higher endosomal pH than MDCK cells (Murakami et al., 2012). Despite the relatively lower replication capacity of both the wild-type and mutant viruses in Vero cells compared to Calu-3 or MDCK cells, both viruses exhibited productive replication and peaked at $\geq 10^{4.6}$ EID_{50}/ml (Fig. 6A). At 72 h p.i., peak titers were significantly higher ($p < 0.05$) for the mutant HA2-K64E virus compared to wild-type, suggesting that the mutant virus, which possesses a higher threshold pH for HA activation, has an advantage for replicating in cells with a higher endosomal pH.

The irreversible conformational changes of HA proteins induced by exposure to low pH can also be triggered by exposure to heat at neutral pH (Ruigrok et al., 1986). For certain influenza viruses, enhanced virus acid stability is exhibited along with improved stability at higher temperatures or prolonged maintenance of infectivity at ambient temperatures (Ruigrok et al., 1986; Scholtissek, 1985). Therefore, we next compared the stability of wild-type and HA2-K64E mutant viruses under various conditions. To compare virus stability at high temperature, aliquots of 75 μl of wild-type or HA2-K64E mutant virus were incubated in a 56 °C water bath; we found that the HA2-K64E mutant virus completely lost hemagglutination activity after 3 h, whereas the wild-type virus maintained hemagglutination activity beyond 6 h at this temperature (Fig. 6B). We next compared virus stability by incubating 75 μl aliquots of wild-type or HA2-K64E mutant virus in an environmental chamber set at 20 °C and 50% relative humidity. Wild-type virus generally maintained higher titers (approximately one log) compared to the HA2-K64E mutant virus for over a month at this room temperature setting (Fig. 6C).

Influenza virus persistence on fomites under ambient laboratory conditions was assessed by depositing 10 μl of virus into 96-well plates. After the suspensions were allowed to evaporate (approximately 3 h at room temperature), the plates were transferred to an incubator set at 20 °C and 50% relative humidity, and then virus infectivity was examined over time. Both viruses started with comparable titers at 0 h and gradually lost infectivity over 6 days, at which point only residual infectious virus was detected (Fig. 6D). The wild-type virus maintained a higher mean titer (~2 logs) for 1–3 days compared with the HA2-K64E mutant virus ($p < 0.001$); after 4 days, the difference in titers dropped to approximately 1 log ($p < 0.05$). Our findings suggest that the recombinant wild-type virus exhibits a higher capacity for persistence in fomites compared to the HA2-K64E mutant virus. Taken together, we conclude that the single K residue at HA2–64 in the TW/17 virus

HA not only modulates virus threshold pH for HA activation, but also affects virus replication capacity, virus heat stability, and persistence on fomites.

Both the 4-aa cleavage site insertion and HA2-K64 of the HPAI A(H7N9) virus contribute to virulence in mice.

The HA has been recognized as a primary virulence determinant for influenza viruses; both HA cleavability and virus acid stability have been linked to virulence in animal models (Russell et al., 2018; Steinhauer, 1999). In order to investigate the residues in the HPAI TW/17 virus HA that contribute to virus pathogenicity, we compared virulence in a mouse model of the recombinant PR8 virus with wild-type TW/17 virus HA and three mutant viruses (HA2-K64E, HA1-Del321-324/R320G, and HA1-R320G). A recombinant PR8 virus with the wild-type HA and NA from LPAI AH/13 virus was included as a control. Groups of five mice were inoculated with 10-fold serially diluted recombinant viruses, and were monitored daily for morbidity and mortality. We found that both wild-type and two mutant viruses (HA2-K64E and HA1-R320G) caused lethal infection in mice with comparable 50% mouse lethal dose (MLD_{50}) values of 3.5 $\log_{10}$ EID_{50}. However, the mutant virus (HA1-Del321-324/R320G) was attenuated and exhibited an MLD_{50} value of 4.4 $\log_{10}$ EID_{50}. As a control, the recombinant virus with the AH/13 virus HA possessed reduced virulence (MLD_{50} of 5.5). Additionally, although all groups of mice inoculated with $10^{3.0}$ EID_{50} of virus survived the infection, they exhibited varying degrees of morbidity (Fig. 7A). Mice inoculated with the mutant viruses, HA2-K64E or HA1-Del321-324/R320G, experienced significantly reduced weight loss compared to mice inoculated with wild-type or the mutant virus, HA1-R320G. We next compared virus replication in mouse tissues after inoculation with either a high dose ($10^{6.0}$ EID_{50}) or low dose ($10^{2.0}$ EID_{50}) of wild-type or mutant viruses. On day 3 p.i., no significant differences in titers were observed among the virus groups receiving the same dose. However, by 6 days p.i., the high dose mutant virus (HA1-Del321-324/R320G) group and the low dose mutant virus (HA2-K64E) group exhibited significantly reduced viral titers on day 6 p.i. (Fig. 7B). Similar to wild-type HPAI or LPAI A(H7N9) viruses, none of the recombinant viruses was able to replicate in murine brain tissue at high or low inoculum doses. Taken together, we conclude that both the 4-aa cleavage site insertion and HA2-K64 contribute to the high virulence phenotype of TW/17 virus, whereas the additional basic residue at HA1-R320 of the cleavage site has a minimal effect on TW/17 virus virulence in the mouse model.

3. Discussion

Avian influenza A(H7N9) viruses represent an ongoing threat to both public health and the poultry industry since their first detection in China in 2013. Rapid evolution led to emergence of HPAI A(H7N9) viruses during the fifth-wave of A(H7N9) human epidemics, causing outbreaks in poultry farms and human infections. It is imperative to understand how viruses such as A(H7N9) evolve to gain enhanced virulence and pandemic potential. By comparing the sequences of LPAI and HPAI A(H7N9) viruses combined with both *in vitro* and *in vivo* approaches, we identified key residues, which naturally emerged in HPAI A(H7N9) viruses and that are involved in HA intracellular cleavage, acid stability, and virulence in a mammalian model. Although the enhanced acid stability among HPAI

A(H7N9) viruses has not yet increased virus transmissibility in the ferret model, close monitoring of such changes during surveillance activities will improve pandemic preparedness.

The HA cleavage property is the main determinant of avian influenza virus virulence in chickens. All of the HPAI A(H7N9) isolates that have been tested were highly pathogenic in chickens; however, they exhibited substantial differences regarding their virulence in mammalian animal models, with HPAI A(H7N9) human isolates seemingly more virulent than those isolated from chickens or the environment (Shi et al., 2018). In our study, we focused on the HA from a previously well-characterized human HPAI isolate (TW/17), which has been shown to be highly virulent in mice, and demonstrate that the 4-aa insertion is essential for its intracellular cleavage. Furthermore, although the substitution HA1-G320R adjacent to the amino-terminus of the insertion is more prevalent in HPAI A(H7N9) human isolates than in the viruses isolated from non-human specimens, we found that this substitution had a minimal effect on TW/17 virus HA cleavage in 293T cells. Moreover, the recombinant virus bearing the HA1-R320G mutation exhibited comparable morbidity, mortality, and replication capacity in mice to the recombinant virus with a wild-type HA. These results indicate that the disparity at position HA1–320 between human- and non-human-origin HPAI A(H7N9) viruses is not the main determinant for the differences observed in murine pathogenicity, which points to other substitutions that have emerged during virus replication in humans to enhance mammalian virulence. In contrast to the dispensable role of HA1-R320 in virulence, the 4-aa insertion at the HA cleavage site of TW/17 virus was shown to contribute to high virulence. Overall, our study suggests that the 4-aa insertion acquired during A(H7N9) virus evolution from low to high virulence in chickens also contributes to a highly pathogenic phenotype in the mouse model. However, the additional mutation adjacent to the amino-terminus of the insertion has no significant effect on viral virulence in mice, emphasizing that mammalian pathogenicity of avian influenza viruses is a multifactorial trait, warranting further investigation to fully understand the virulence of HPAI A(H7N9) viruses in mammals.

Influenza viruses have exhibited substantial differences in the threshold pH for HA activation ranging from pH values of 4.8–6.2 (Russell et al., 2018); viruses possessing a lower threshold pH for fusion are often referred to as more acid stable. A wide range of residues throughout the HA head and stem domain have been identified to modulate the pH for HA activation with a certain degree of strain or subtype specificity (Russell et al., 2018). With regard to the enhanced acid stability of HPAI A(H7N9) viruses identified in our previous report (Sun et al., 2018), in this study, we revealed that a single, conserved residue HA2-K64, shared by both human and avian isolates of HPAI A(H7N9) viruses, was responsible for the reduced fusion activation pH, and that the single mutation, HA2-K64E, in the recombinant mutant HPAI TW/17 virus was sufficient to shift fusion pH from 5.4 to 5.8. In a previous study of LPAI AH/13 virus, the substitutions L217Q (H7 numbering), located in the HA receptor binding site, HA1-N94K (H7 numbering), located at the trimer interface, and HA2-K58I, located at the top of a short α-helix, were found to enhance acid stability. Each of these three single mutations was shown to reduce the AH/13 virus fusion threshold by approximately 0.2–0.6 pH units (Schrauwen et al., 2016). Interestingly, wild-type TW/17 virus already has Q217 (H7 numbering) in the HA, and the Q217L mutation

had no detectable effect on HA activation pH in our study, indicating that this residue is not a determinant of the reduced threshold pH for fusion of HPAI A(H7N9) viruses. With regard to HA1-N94K and HA2-K58I, none of the HPAI A(H7N9) viruses sequenced to date has acquired mutations at these positions, suggesting that these mutations may not have sufficient fitness during A(H7N9) evolution in chicken or mammalian hosts. In summary, for the first time, we are able to show that the naturally emerging residue, HA2-K64, which is shared by HPAI A(H7N9) viruses, is critical for virus acid stability.

There is increasing evidence that influenza virus acid stability contributes to virus tropism, virulence, and airborne transmission (Russell et al., 2018). Previous studies with H5 avian influenza viruses showed that HPAI viruses tend to have a relatively higher HA activation pH compared to closely related H5 viruses of low pathogenicity, and suggested that H5 influenza viruses with a higher HA activation pH are favored in terms of efficient virus replication and transmission in chickens (DuBois et al., 2011). Interestingly, HPAI A(H7N9) virus appears to be more acid stable than LPAI A(H7N9) virus, which may reflect subtype or strain specific differences. Whether acid stability of A(H7N9) virus contributes to virulence and transmission in chickens would need further investigation. Moreover, virus acid stability has been shown to contribute to virulence and host adaptation in mammals, although both attenuation and exacerbation of virulence in the mouse model has been observed for acid-stabilizing mutations in A(H5N1) viruses (Zaraket et al., 2013; Koerner et al., 2012). In our study, by using two isogeneic recombinant A(H7N9) viruses bearing a single HA2-K64E mutation with a threshold pH of 5.4 or 5.8, respectively, we found that the A(H7N9) virus with a lower threshold pH exhibited increased replication capacity in murine lung tissues, especially at a lower inoculum dose. However, whether this substitution affects virus virulence in other mammalian species requires further study. A(H7N9) virus with a lysine residue at position HA2–64 exhibited better environmental stability. Prolonged persistence of infectious influenza viruses in the environment, either in an aerosol state or on fomites, may improve the likelihood of virus transmissibility to susceptible hosts. Additionally, improved stability of influenza virus may be applicable to better design and development of A(H7N9) vaccines. Lastly, the two A(H7N9) recombinant viruses that fuse at differing pH values also exhibited differences in viral replication in cells with a relatively higher endosomal pH. However, due to the high complexity and heterogeneity of cells lining the respiratory tract of mammalian species, further comprehensive study is required to better assess how HA activation pH affects replication *in vivo* at the sites of virus entry and spread.

One of the major public health concerns for A(H7N9) virus is that the virus may acquire the ability to transmit through the air. However, although HPAI A(H7N9) viruses have exhibited enhanced virulence and acid stability with concurrent environmental stability, the viruses have not yet demonstrated this ability. We suspect that the dominant avian receptor binding specificity of HPAI A(H7N9) viruses may be one of the major obstacles for airborne transmission. Although the recent widely implemented poultry vaccination program has substantially reduced virus spread in China, A(H7N9) viruses continue to evolve and may exhibit a different evolutionary dynamic under vaccination pressure (Shi et al., 2018; Zeng et al., 2018). Meanwhile, A(H7N9) viruses with higher acid and environmental stability may also potentially drive virus evolution toward enhanced transmissibility. Overall, our study has identified key residues in the HA of HPAI A(H7N9) viruses that are involved in

virulence and stability, which may prove to be predictive of an H7 strain capable of causing a pandemic. Continued surveillance and monitoring of the emerging A(H7N9) viruses with these molecular markers along with subsequent phenotypic characterizations and risk assessments are critical for pandemic preparedness.

4. Materials and methods

Cells and plasmids.

All cells including 293T, Calu-3, Vero, and Madin-Darby canine kidney-London (MDCK) were obtained from the Scientific Resources Program, Centers for Disease Control and Prevention (CDC; Atlanta, GA) and were maintained in Dulbecco's modified Eagle's medium (DMEM) or Eagle's minimal essential medium (MEM) medium with 10% fetal bovine serum (FBS) as described previously (Zeng et al., 2007). The genes encoding the HA and NA proteins of TW/17 and AH/13 virus were synthesized by Genscript (Piscataway, NJ) and subsequently cloned into the bidirectional pDZ vector as described previously (Martinez-Sobrido and Garcia-Sastre, 2010). The Agilent QuikChange site-directed mutagenesis kit (Santa Clara, CA) was used to generate mutations at the targeted sites in the pDZ-TW/HA backbone. The plasmids encoding the six internal gene segments (PB1, PB2, PA, NP, NS, and M) of A/Puerto Rico/8/1934 (PR8) virus in the pDZ vector were kindly provided by Adolfo Garcia-Sastre, Mount Sinai School of Medicine, New York and were used for recombinant virus rescue.

HA expression and cleavage in 293T cells.

Cultures of 293T cells grown on 6-well plates were transfected with 800 ng of each plasmid encoding wild-type or mutant forms of TW/17 virus HA and 200 ng of pDZ-PR8-M along with 3 μl of Lipofectamine (2000) (Thermo Fisher Scientific) for 48 h before cell surface proteins were labeled with biotin followed by streptavidin bead immunoprecipitation as described previously (Sun et al., 2016). HA expression on the cell surface and intracellular cleavage were examined by SDS-PAGE followed by Western blot analysis using rabbit *anti*-H7 HA polyclonal antibody (Sino Biological, Cat# 40103-RP02, PA) and HRP-conjugated anti-rabbit antibody (Thermo Fisher Scientific).

Recombinant virus rescue, propagation, and growth kinetics.

Recombinant PR8 viruses with HA (wild-type or mutant forms) and NA from TW/17 or AH/13 virus, and the internal genes from PR8, were rescued by transfecting 293T cells as described previously (Martinez-Sobrido and Garcia-Sastre, 2010). The rescued recombinant viruses were then propagated in the allantoic cavity of 10-day-old embryonated hens' eggs at 37 °C for 36–48 h, and viral titers were determined by titration in eggs and were expressed as the 50% egg infectious dose (EID_{50}) per ml using the method of Reed and Muench (Reed LJ, 1938). Stock viruses were confirmed by sequencing and were tested for exclusivity and sterility to ensure lack of contamination with other subtypes of viruses or bacteria. Viral replication *in vitro* was evaluated in Calu-3, MDCK, and Vero cells. In brief, cells grown in 6-well plates were inoculated with recombinant PR8:TW/17-HA/NA virus (wild-type or mutant) at an MOI of 0.01 EID_{50}, and were cultured at 37 °C in virus infection medium, DMEM (for Vero and MDCK cells) or MEM (for Calu-3 cells) supplemented with

0.3% BSA. Viral titers of cell culture supernatants collected at 2, 24, 48, 72, and 96 h p. i. were determined by titration in eggs and expressed as $\log_{10}$ EID_{50}/ml. Limit of detection was $10^{1.5}$ EID_{50}/ml.

Syncytia formation assay to evaluate the threshold pH of HA activation.

Vero cells grown in 12-well plates were transfected with plasmids expressing wild-type or mutant HAs of TW/17 virus or the wild-type HA of AH/13 virus for 48 h, or were inoculated with recombinant PR8:TW-HA/NA (wild-type or mutant) at an MOI of 1 for 16 h. Vero cell cultures were then treated with 5 pg/ml of N-tosyl-L-phenylalanine chloromethyl ketone (TPCK)-trypsin at 37 °C for 15 min. To induce syncytia formation, cells were incubated with fusion buffer (20 mM HEPES, 2 mM $CaCl_2$, 150 mM NaCl, 20 mM citric acid monohydrate/sodium citrate tribasic dehydrate) with the pH adjusted to 5.2, 5.4, 5.6, 5.8 or 6.0 for 5 min at 37 °C. At 3h post fusion induction, syncytia were visualized by immunofluorescence microscopy after staining the cells with rabbit *anti*-H7 HA monoclonal antibody (Sino Biological, Cat#11082-R002, PA) and Alexa Fluor™ 488-labeled anti-rabbit IgG secondary antibody (Thermo Fisher Scientific), and diamidino-2-phenylindole (DAPI) for nuclei. The pH threshold for fusion was defined as the highest representative pH value from three replicates at which at least 50% syncytia formation were observed among HA-positive cells.

Heat stability and environmental persistence.

Aliquots (75 μl each) of comparable amounts of recombinant PR8:TW/17-HA/NA viruses (wild-type or mutant) were placed in 1.5 ml Eppendorf tubes and incubated, in triplicate, at 56 °C using a water bath or at 20 °C and 50% relative humidity in a Microclimate MCBHS-1.2 environmental chamber (Cincinnati Sub-Zero) for various lengths of time as indicated. Virus integrity after incubation at 56 °C was evaluated by a hemagglutinatin assay with turkey red blood cells and virus infectivity was assayed after incubation at 20 °C by titration in eggs. To assess virus persistence on fomites, 10 μl of stock virus (six replicates for each time point) were deposited onto 96-well plates and allowed to evaporate (approximately 3 h) before the plates were transferred to a Microclimate environmental chamber maintained at 20 °C and 50% relative humidity. Virus in each well was reconstituted with 60 μl of phosphate-buffered saline (PBS) at various time points (0, 1, 3, 4, and 6 days) and were immediately stored at −80 °C until titration in eggs.

Mouse infection.

Animal experiments were performed under the guidance of the Centers for Disease Control and Prevention Institutional Animal Care and Use Committee and were conducted in an Association for Assessment and Accreditation of Laboratory Animal Care International-accredited animal facility. Experiments were performed in Biosafety level-3 containment including enhancements (BSL-3E) required by the U.S. Department of Agriculture and Select Agent Program outlined in Biosafety in Microbiological and Biomedical Laboratories (Chosewood, 2009). Groups of five 6- to 8-week-old female BALB/c mice (Charles River Laboratories, Wilmington, MA) were inoculated intranasally with 50 μl of serial 10-fold dilutions of PR8:TW/17-HA/NA virus (wild-type or mutants) or PR8:AH/13-HA/NA virus, ranging from $10^{3.0}$ to $10^{6.0}$ EID_{50} diluted in PBS. The inoculated mice were observed for 14

days to monitor morbidity (measured by weight loss) and mortality; any mouse exhibiting ≥25% pre-inoculation weight loss was euthanized. In addition, groups of six mice were intranasally inoculated with 50 μl of $10^{2.0}$ or $10^{6.0}$ EID_{50} of PR8:TW/17-HA/NA virus (wild-type or mutants) to compare viral replication in lung tissues on day 3 p. i. (n = 3) or in both lung and brain tissues on day 6 p. i (n = 3).

Acknowledgements

We thank the Comparative Medicine Branch for excellent care of the animals used in this study. The findings and conclusions in this report are those of the authors and do not necessarily represent the views of the Centers for Disease Control and Prevention or the Agency for Toxic Substances and Disease Registry. Hannah M. Creager was supported by the Oak Ridge Institute for Science and Education.

References

Alvarado-Facundo E, Gao Y, Ribas-Aparicio RM, Jimenez-Alberto A, Weiss CD, Wang W, 2015 Influenza virus M2 protein ion channel activity helps to maintain pandemic 2009 H1N1 virus hemagglutinin fusion competence during transport to the cell surface. J. Virol 89, 1975–1985. [PubMed: 25473053]

Belser JA, Gustin KM, Pearce MB, Maines TR, Zeng H, Pappas C, Sun X, Carney PJ, Villanueva JM, Stevens J, Katz JM, Tumpey TM, 2013 Pathogenesis and transmission of avian influenza A(H7N9) virus in ferrets and mice. Nature 501, 556–559. [PubMed: 23842497]

Belser JA, Creager HM, Sun X, Gustin KM, Jones T, Shieh WJ, Maines TR, Tumpey TM, 2016 Mammalian pathogenesis and transmission of H7N9 influenza viruses from three waves, 2013-2015. J. Virol 90, 4647–4657. [PubMed: 26912620]

Bottcher-Friebertshauser E, Stein DA, Klenk HD, Garten W, 2011 Inhibition of influenza virus infection in human airway cell cultures by an antisense peptide-conjugated morpholino oligomer targeting the hemagglutinin-activating protease TMPRSS2. J. Virol 85, 1554–1562. [PubMed: 21123387]

CDC, 2018 Asian Lineage Avian Influenza A(H7N9) Virus. https://www.cdc.gov/flu/avianflu/h7n9-virus.htm, Accessed date: 15 November 2018.

Chosewood LCWD, 2009 Biosafety in Microbiological and Medical Laboratories, fifth ed. U. S. Department of Health and Human Services, Centers for Disease Control and Prevention, National Institutes of Health, Washington, DC.

DuBois RM, Zaraket H, Reddivari M, Heath RJ, White SW, Russell CJ, 2011 Acid stability of the hemagglutinin protein regulates H5N1 influenza virus pathogenicity. PLoS Pathog. 7, e1002398. [PubMed: 22144894]

FAO, 2019 H7N9 Situation Update, http://www.fao.org/ag/againfo/programmes/en/empres/H7N9/situation_update.html, Accessed date: 25 February 2019.

Fields BN, Knipe DM, Howley PM, 2007 Fields Virology. Wolters Kluwer Health/Lippincott Williams & Wilkins, Philadelphia.

Gao R, Cao B, Hu Y, Feng Z, Wang D, Hu W, Chen J, Jie Z, Qiu H, Xu K, Xu X, Lu H, Zhu W, Gao Z, Xiang N, Shen Y, He Z, Gu Y, Zhang Z, Yang Y, Zhao X, Zhou L, Li X, Zou S, Zhang Y, Li X, Yang L, Guo J, Dong J, Li Q, Dong L, Zhu Y, Bai T, Wang S, Hao P, Yang W, Zhang Y, Han J, Yu H, Li D, Gao GF, Wu G, Wang Y, Yuan Z, Shu Y, 2013 Human infection with a novel avian-origin influenza A(H7N9) virus. N. Engl. J. Med 368, 1888–1897. [PubMed: 23577628]

Hatta M, Gao P, Halfmann P, Kawaoka Y, 2001 Molecular basis for high virulence of Hong Kong H5N1 influenza A viruses. Science 293, 1840–1842. [PubMed: 11546875]

Ke C, Mok CKP, Zhu W, Zhou H, He J, Guan W, Wu J, Song W, Wang D, Liu J, Lin Q, Chu DKW, Yang L, Zhong N, Yang Z, Shu Y, Peiris JSM, 2017 Human infection with highly pathogenic avian influenza A(H7N9) virus, China. Emerg. Infect. Dis 23, 1332–1340. [PubMed: 28580899]

Koerner I, Matrosovich MN, Haller O, Staeheli P, Kochs G, 2012 Altered receptor specificity and fusion activity of the haemagglutinin contribute to high virulence of a mouse-adapted influenza A virus. J. Gen. Virol 93, 970–979. [PubMed: 22258863]

Martinez-Sobrido L, Garcia-Sastre A, 2010 Generation of recombinant influenza virus from plasmid DNA. J. Vis. Exp 10.3791/2057.

Murakami S, Horimoto T, Ito M, Takano R, Katsura H, Shimojima M, Kawaoka Y, 2012 Enhanced growth of influenza vaccine seed viruses in vero cells mediated by broadening the optimal pH range for virus membrane fusion. J. Virol 86, 1405–1410. [PubMed: 22090129]

Qi W, Jia W, Liu D, Li J, Bi Y, Xie S, Li B, Hu T, Du Y, Xing L, Zhang J, Zhang F, Wei X, Eden JS, Li H, Tian H, Li W, Su G, Lao G, Xu C, Xu B, Liu W, Zhang G, Ren T, Holmes EC, Cui J, Shi W, Gao GF, Liao M, 2018 Emergence and adaptation of a novel highly pathogenic H7N9 influenza virus in birds and humans from a 2013 human-infecting low-pathogenic ancestor. J. Virol 92.

Reed LJ HM, 1938 A simple method of estimating fifty percent endpoints. J. Hyg 27, 493–497.

Richard M, Schrauwen EJ, de Graaf M, Bestebroer TM, Spronken MI, van Boheemen S, de Meulder D, Lexmond P, Linster M, Herfst S, Smith DJ, van den Brand JM, Burke DF, Kuiken T, Rimmelzwaan GF, Osterhaus AD, Fouchier RA, 2013 Limited airborne transmission of H7N9 influenza A virus between ferrets. Nature 501, 560–563. [PubMed: 23925116]

Ruigrok RW, Martin SR, Wharton SA, Skehel JJ, Bayley PM, Wiley DC, 1986 Conformational changes in the hemagglutinin of influenza virus which accompany heat-induced fusion of virus with liposomes. Virology 155, 484–497. [PubMed: 3788061]

Russell CJ, Hu M, Okda FA, 2018 Influenza hemagglutinin protein stability, activation, and pandemic risk. Trends Microbiol. 26, 841–853. [PubMed: 29681430]

Scholtissek C, 1985 Stability of infectious influenza A viruses to treatment at low pH and heating. Arch. Virol 85, 1–11. [PubMed: 4015405]

Schrauwen EJ, Richard M, Burke DF, Rimmelzwaan GF, Herfst S, Fouchier RA, 2016 Amino acid substitutions that affect receptor binding and stability of the hemagglutinin of influenza A/H7N9 virus. J. Virol 90, 3794–3799. [PubMed: 26792744]

Shi J, Deng G, Ma S, Zeng X, Yin X, Li M, Zhang B, Cui P, Chen Y, Yang H, Wan X, Liu L, Chen P, Jiang Y, Guan Y, Liu J, Gu W, Han S, Song Y, Liang L, Qu Z, Hou Y, Wang X, Bao H, Tian G, Li Y, Jiang L, Li C, Chen H, 2018 Rapid evolution of H7N9 highly pathogenic viruses that emerged in China in 2017. Cell Host Microbe 24, 558–568 e7. [PubMed: 30269969]

Shiryaev SA, Chernov AV, Golubkov VS, Thomsen ER, Chudin E, Chee MS, Kozlov IA, Strongin AY, Cieplak P, 2013 High-resolution analysis and functional mapping of cleavage sites and substrate proteins of furin in the human proteome. PLoS One 8, e54290. [PubMed: 23335997]

Short KR, Richard M, Verhagen JH, van Riel D, Schrauwen EJ, van den Brand JM, Manz B, Bodewes R, Herfst S, 2015 One health, multiple challenges: the inter-species transmission of influenza A virus. One Health 1, 1–13. [PubMed: 26309905]

Steinhauer DA, 1999 Role of hemagglutinin cleavage for the pathogenicity of influenza virus. Virology 258, 1–20. [PubMed: 10329563]

Sun X, Belser JA, Tumpey TM, 2016 A novel eight amino acid insertion contributes to the hemagglutinin cleavability and the virulence of a highly pathogenic avian influenza A (H7N3) virus in mice. Virology 488, 120–128. [PubMed: 26629952]

Sun X, Belser JA, Pappas C, Pulit-Penaloza JA, Brock N, Zeng H, Creager HM, Le S, Wilson M, Lewis A, Stark TJ, Shieh WJ, Barnes J, Tumpey TM, Maines TR, 2018 Risk assessment of fifth-wave H7N9 influenza A viruses in mammalian models. J. Virol 10.1128/JVI.01740-18.

Takeuchi K, Lamb RA, 1994 Influenza virus M2 protein ion channel activity stabilizes the native form of fowl plague virus hemagglutinin during intracellular transport. J. Virol 68, 911–919. [PubMed: 7507186]

Thomas G, 2002 Furin at the cutting edge: from protein traffic to embryogenesis and disease. Nat. Rev. Mol. Cell Biol 3, 753–766. [PubMed: 12360192]

Tong S, Zhu X, Li Y, Shi M, Zhang J, Bourgeois M, Yang H, Chen X, Recuenco S, Gomez J, Chen LM, Johnson A, Tao Y, Dreyfus C, Yu W, McBride R, Carney PJ, Gilbert AT, Chang J, Guo Z, Davis CT, Paulson JC, Stevens J, Rupprecht CE, Holmes EC, Wilson IA, Donis RO, 2013 New world bats harbor diverse influenza A viruses. PLoS Pathog. 9, e1003657. [PubMed: 24130481]

Watanabe T, Kiso M, Fukuyama S, Nakajima N, Imai M, Yamada S, Murakami S, Yamayoshi S, Iwatsuki-Horimoto K, Sakoda Y, Takashita E, McBride R, Noda T, Hatta M, Imai H, Zhao D, Kishida N, Shirakura M, de Vries RP, Shichinohe S, Okamatsu M, Tamura T, Tomita Y, Fujimoto

N, Goto K, Katsura H, Kawakami E, Ishikawa I, Watanabe S, Ito M, Sakai-Tagawa Y, Sugita Y, Uraki R, Yamaji R, Eisfeld AJ, Zhong G, Fan S, Ping J, Maher EA, Hanson A, Uchida Y, Saito T, Ozawa M, Neumann G, Kida H, Odagiri T, Paulson JC, Hasegawa H, Tashiro M, Kawaoka Y, 2013 Characterization of H7N9 influenza A viruses isolated from humans. Nature 501, 551–555. [PubMed: 23842494]

Watanabe T, Watanabe S, Maher EA, Neumann G, Kawaoka Y, 2014 Pandemic potential of avian influenza A(H7N9) viruses. Trends Microbiol. 22, 623–631. [PubMed: 25264312]

Xiong X, Martin SR, Haire LF, Wharton SA, Daniels RS, Bennett MS, McCauley JW, Collins PJ, Walker PA, Skehel JJ, Gamblin SJ, 2013 Receptor binding by an H7N9 influenza virus from humans. Nature 499, 496–499. [PubMed: 23787694]

Yang L, Zhu W,, Li, Chen M, Wu J, Yu P, Qi S, Huang Y., Shi W, Dong J, Zhao X, Huang W, Li Z, Zeng X, Bo H, Chen T, Chen W, Liu J, Zhang Y, Liang Z, Shi W, Shu Y., Wang D, 2017 Genesis and spread of newly emerged highly pathogenic H7N9 avian viruses in mainland China. J. Virol 91.

Yang H, Carney PJ, Chang JC, Guo Z, Stevens J, 2018 Structural and molecular characterization of the hemagglutinin from the fifth epidemic wave A(H7N9) influenza viruses. J. Virol 10.1128/JVI.00375-18.

Zaraket H, Bridges OA, Russell CJ, 2013 The pH of activation of the hemagglutinin protein regulates H5N1 influenza virus replication and pathogenesis in mice. J. Virol 87, 4826–4834. [PubMed: 23449784]

Zeng H, Goldsmith C, Thawatsupha P, Chittaganpitch M, Waicharoen S, Zaki S, Tumpey TM, Katz JM, 2007 Highly pathogenic avian influenza H5N1 viruses elicit an attenuated type i interferon response in polarized human bronchial epithelial cells. J. Virol 81, 12439–12449. [PubMed: 17855549]

Zeng X, Tian G, Shi J, Deng G, Li C, Chen H, 2018 Vaccination of poultry successfully eliminated human infection with H7N9 virus in China. Sci. China Life Sci 10.1007/s11427-018-9420-1.

Zhang F, Bi Y, Wang J, Wong G, Shi W, Hu F, Yang Y, Yang L, Deng X, Jiang S, He X, Liu Y, Yin C, Zhong N, Gao GF, 2017 Human infections with recently-emerging highly pathogenic H7N9 avian influenza virus in China. J. Infect 75, 71–75. [PubMed: 28390707]

Zhou L, Ren R, Yang L, Bao C, Wu J, Wang D, Li C, Xiang N, Wang Y, Li D, Sui H, Shu Y, Feng Z, Li Q, Ni D, 2017 Sudden increase in human infection with avian influenza A(H7N9) virus in China, September-December 2016. Western Pac. Surveill. Response J 8, 6–14.

	HA1-38 (H3:48)	HA1-112 (H3:122)	HA1-164 (H3:173)	HA1-217 (H3:226)	HA1-317 (H3:326)	HA1-320	HA2-64
LPAI H7N9 consensus (733 isolates)	I	T	K	L	I	G	E
HPAI H7N9 consensus (125 isolates)	T	P	E	Q	V	R	K

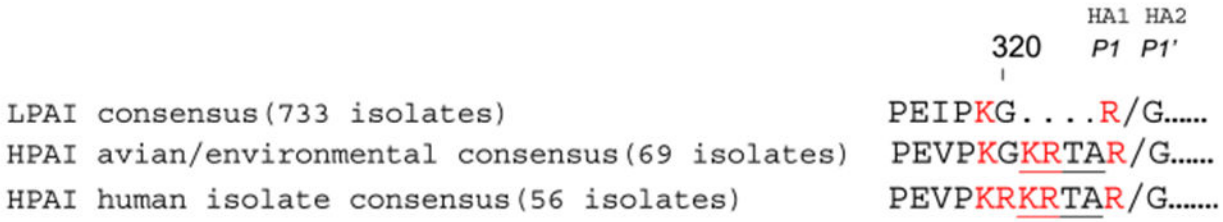

Fig. 1. Sequence analysis of fifth-wave A(H7N9) virus HA proteins.

The amino acid sequences of HA proteins derived from 858 fifth-wave A(H7N9) isolates or passages of isolates (733 LPAI, 125 HPAI, inclusive of 69 avian/environmental isolates and 56 human isolates) were aligned using BioEdit and the positions of differing amino acids are shown. The numbers in parentheses are H3 numbering. Cleavage site consensus sequence comparisons between LPAI and HPAI A(H7N9) viruses of avian/environmental and human isolates are shown with basic residues indicated in red and insertions underlined. The HA cleaves between R and G, corresponding to the P1 and P1′ positions.

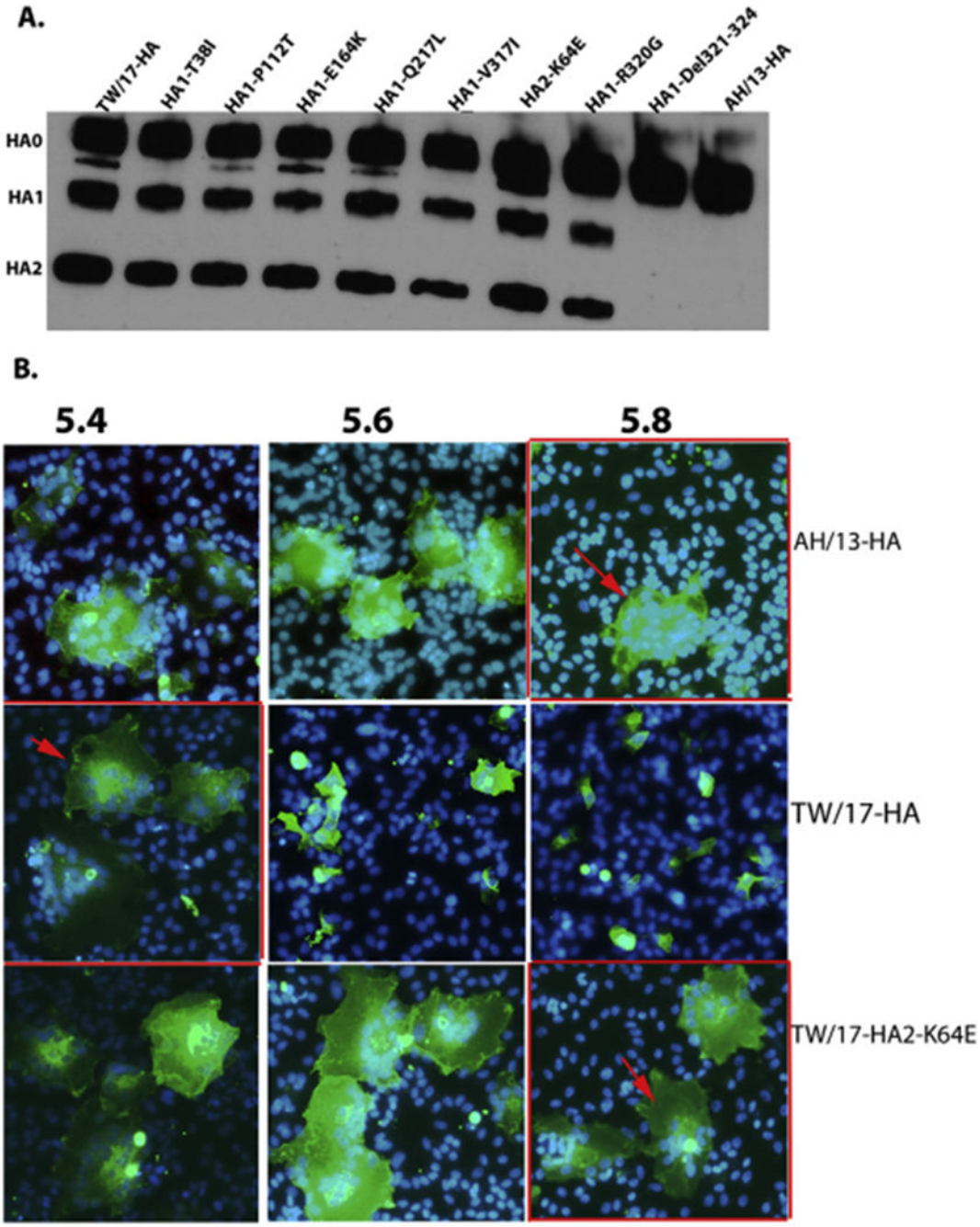

Fig. 2. Cleavage and fusion activity of wild-type and mutant TW/17 virus HA.

(A) Plasmids encoding wild-type or mutant HAs of HPAI TW/17 virus or wild-type LPAI AH/13 virus HA were transfected into 293T cells, and the surface-expressed proteins were biotin-labeled and then pulled down by streptavidin beads. The cleavability of the surface-expressed HA proteins was analyzed by SDS-PAGE and Western blot using rabbit anti-HA polyclonal antibody, which recognizes uncleaved HA0 and the cleaved form of HA (HA1, HA2). (B) Cultures of Vero cells were transfected with the plasmids encoding the HA from AH/13 virus (AH/13-HA) or TW/17 virus (wild-type, TW/17-HA; mutant, TW/17-HA2-

K64E) for 48 h before cells were treated with 5 μg/ml of TPCK-trypsin for 15 min at 37 °C to cleave HA0. To induce syncytia formation, cells were incubated for 5 min with fusion buffers of pH values ranging from 5.2 to 6.0, with 0.2 unit increments, and were visualized 3h later by staining HA proteins (green) and nuclei (blue) and immunofluorescence microscopy. Representative images at pH values of 5.4, 5.6, and 5.8 derived from three replicates are shown. Red arrows indicate syncytia, and the image bordered in red indicates the pH threshold at which 50% of HA-positive cells formed syncytia.

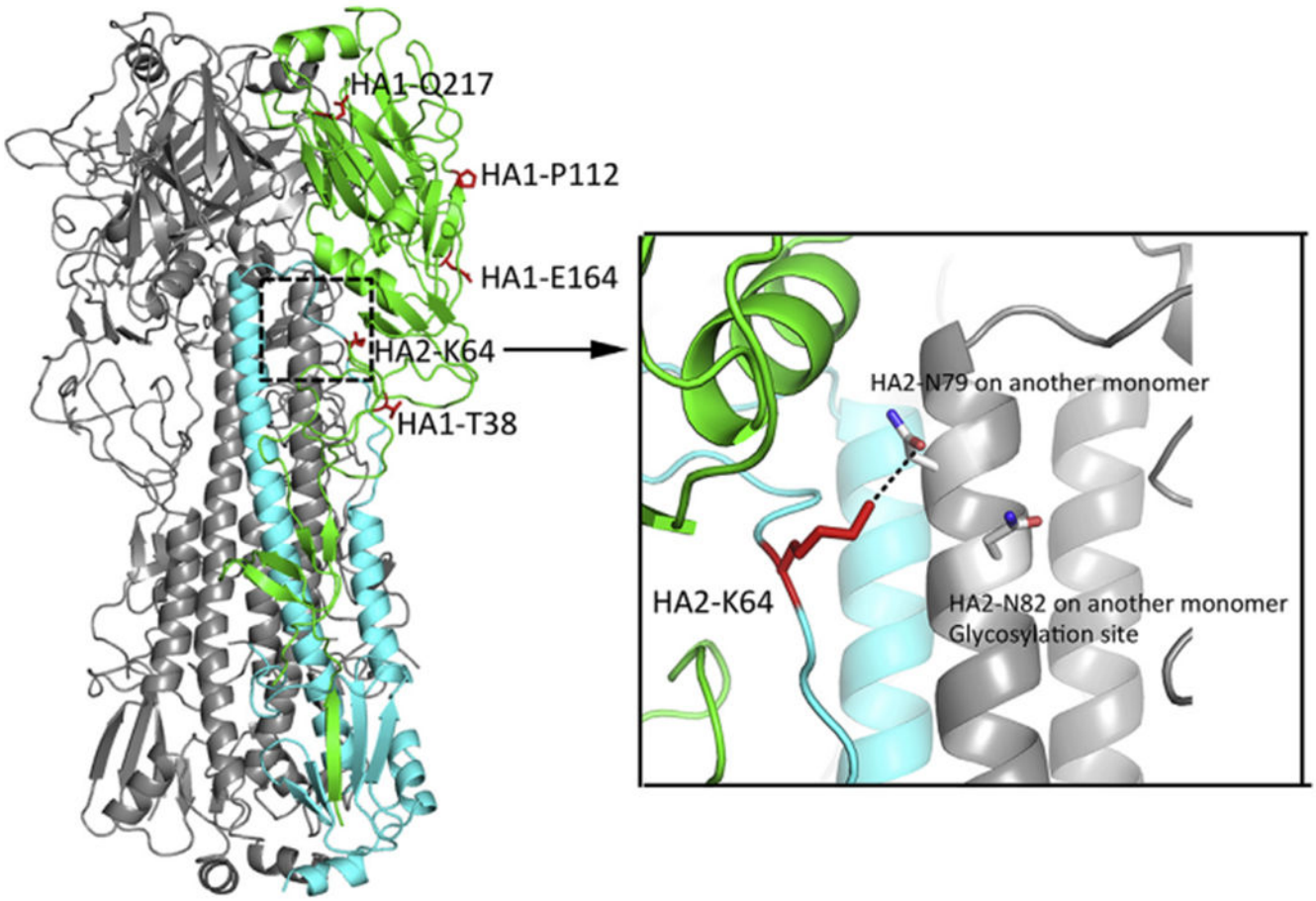

Fig. 3. Structural illustration of TW/17 virus HA protein.

The TW/17 HA trimer was modeled with PyMOL version 2.2.3 from A/Guangdong/17SF003/2016 (PDB ID: 6D7U) with the highlighted residues HA1-(38, 112, 164, 217; H7 numbering), and HA2-64 in one monomer (left) and a close-up image of the residue HA2-K64 forming potential hydrogen bonds with HA2-N79 and the glycans of HA2-N82 from a neighboring monomer (right).

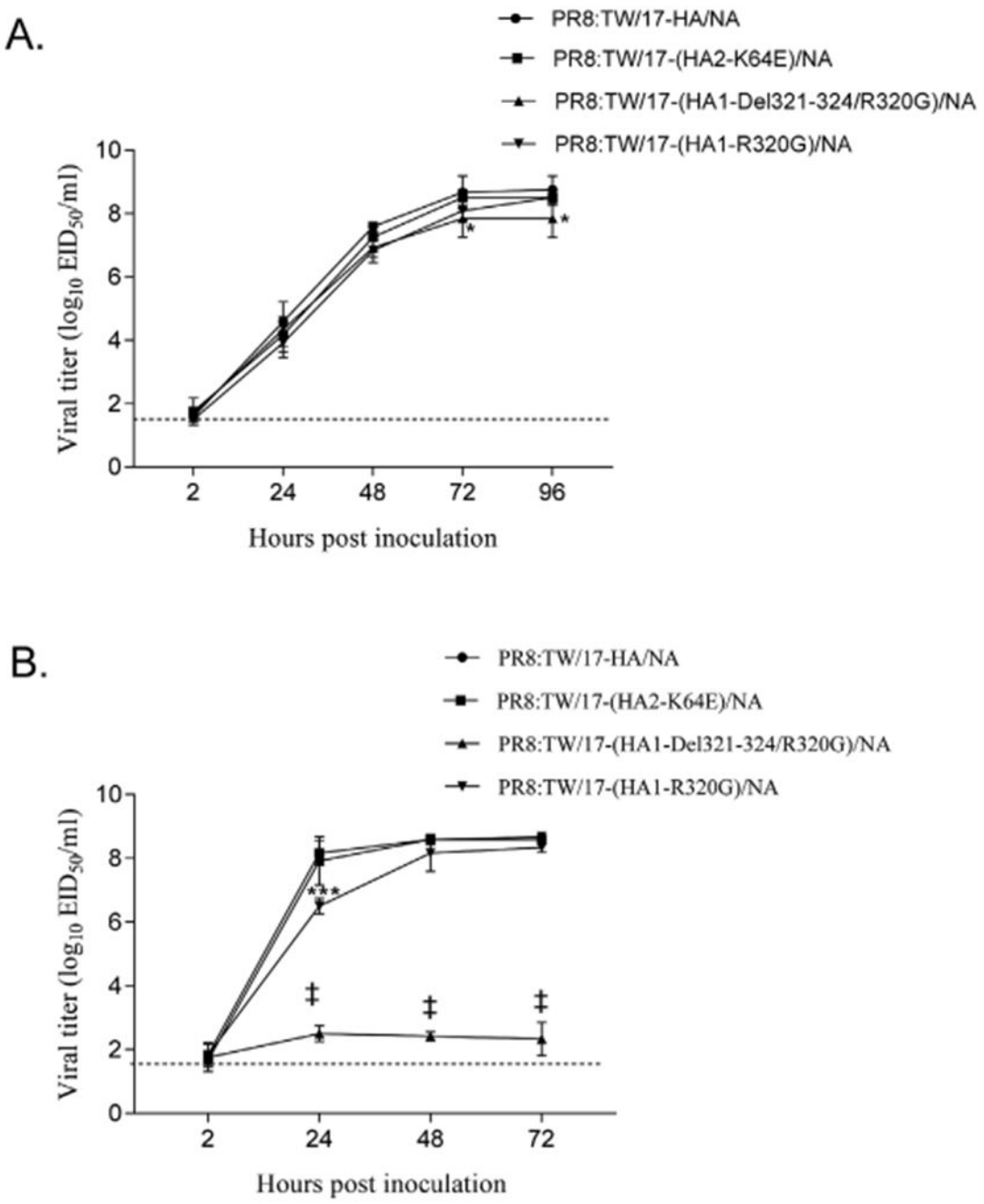

Fig. 4. Replication kinetics of recombinant PR8:TW/17-HA/NA viruses in Calu-3 or MDCK cells.

Calu-3 cells (grown on 24 mm transwells), which produce extracellular proteases, and MDCK cells (grown on 6-well plates), which do not produce extracellular proteases, were inoculated with recombinant PR8 viruses bearing wild-type or mutant HAs of TW/17 virus at an MOI of 0.01 for 1 h followed by incubation with fresh viral infection medium. The supernatants from the infected Calu-3 (A) or MDCK cells (B) were collected at various time points for subsequent viral titer determination in eggs. Viral titers were plotted as the mean with standard deviation (SD) from three independent replicates. The detection limit

indicated by the dashed line was 1.5 $\log_{10}$ EID_{50}/ml. Two-way analysis of variance followed by Dunnett's multiple comparisons test between the wild-type and each of the mutant viruses was performed with GraphPad Prism. *, $p \leq 0.05$; ***, $p \leq 0.001$; ‡, $p \leq 0.0001$.

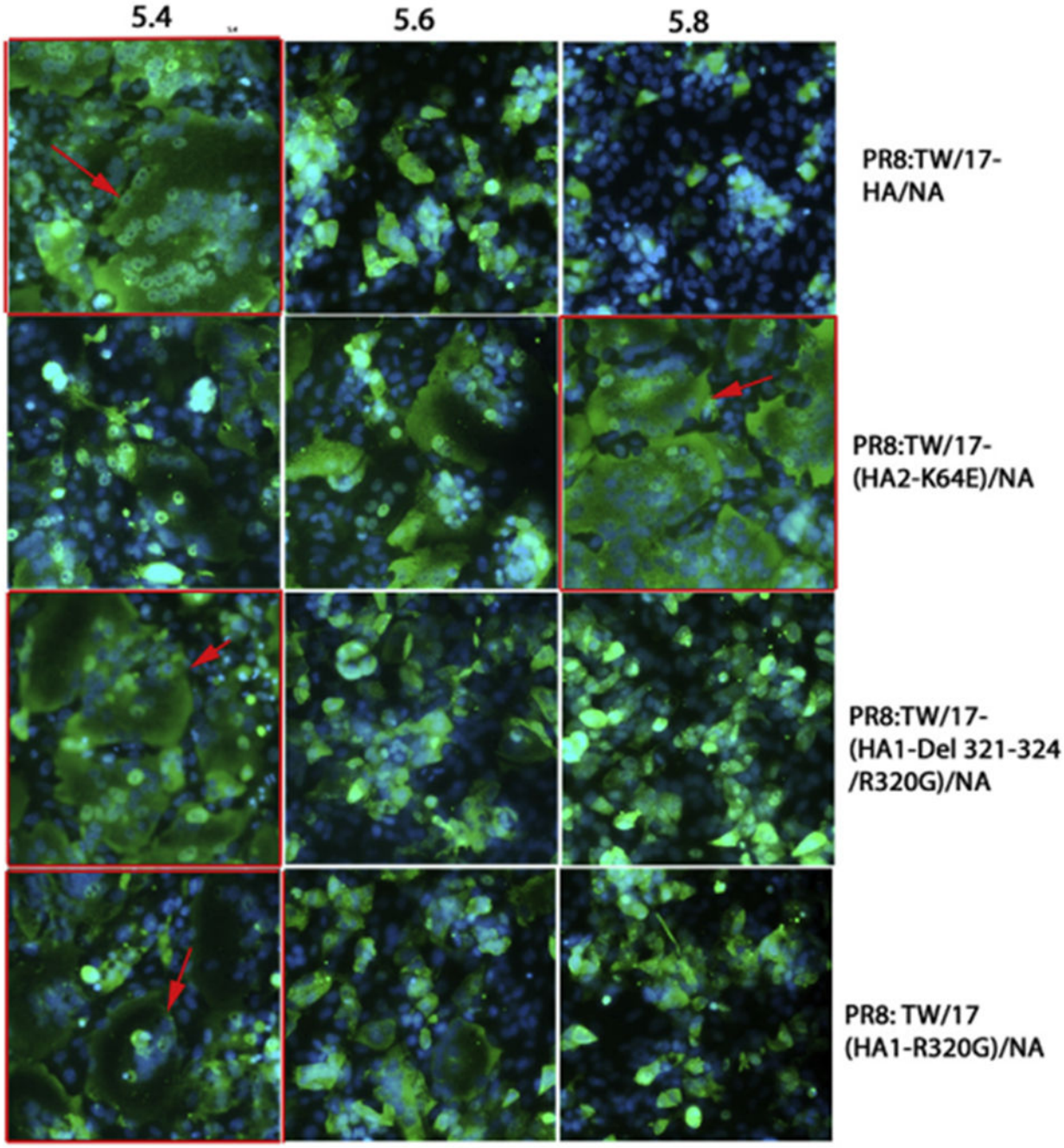

Fig. 5. Syncytia formation induced by recombinant PR8:TW/17-HA/NA viruses in Vero cells.

Cultures of Vero cells were inoculated with recombinant PR8 viruses expressing wild-type or mutant versions of the TW/17 virus HA at an MOI of 1 for 16 h, followed by incubation with 5 μg/ml of TPCK-trypsin for 15 min to cleave expressed HA0. To induce syncytia formation, Vero cells were incubated for 5 min with fusion buffers of pH values ranging from 5.2 to 6.0, with 0.2 unit increments, and were visualized 3 h later by staining HA protein (green) and nuclei (blue) and immunofluorescence microscopy. Representative images at pH values of 5.4, 5.6, and 5.8 derived from three replicates are shown. Red arrows

indicate syncytia, and the image bordered in the red indicates the pH threshold at which 50% of HA-positive cells formed syncytia.

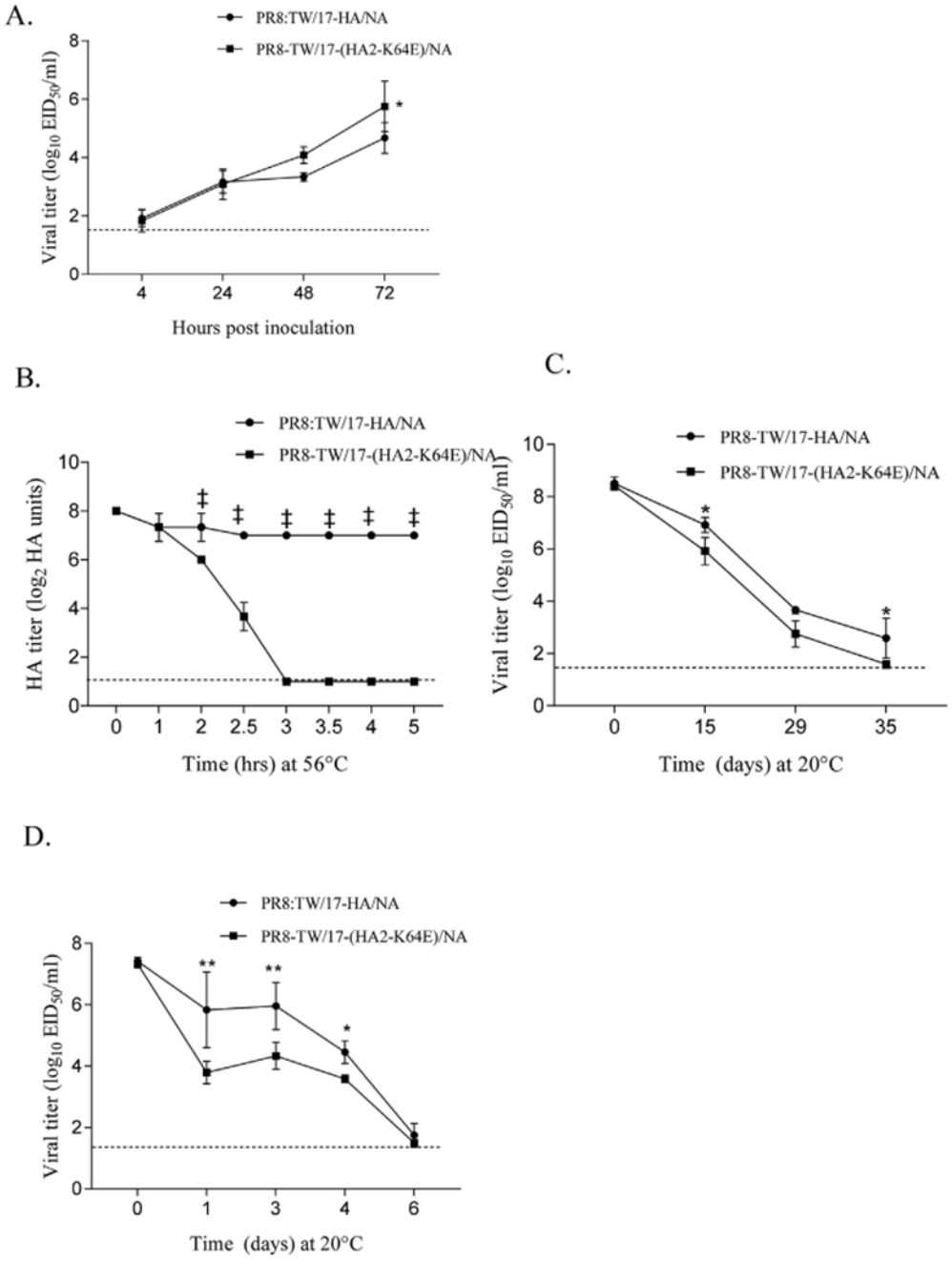

Fig. 6. Replication and stability of wild-type and mutant PR8:TW/17-HA/NA viruses.

(A) Vero cells grown on 6-well-plates were inoculated in triplicate with wild-type or mutant (HA2-K64E) recombinant viruses at an MOI of 0.01 and incubated at 37 °C; supernatants from the cultures were collected at 4, 24, 48, and 72 h p. i. for titration in eggs and are expressed as the mean $\log_{10}$ EID_{50}/ml with standard deviation (SD). (B) Mean hemagglutination titers ($\log_2$ with SD) are presented from three replicates of the wild-type or mutant viruses after incubation at 56 °C for the indicated times. (C) Wild-type and mutant viruses (75 μl) were incubated in triplicate at 20 °C and 50% relative humidity for the

indicated times. Viral titers were determined in eggs and are expressed as the mean $\log_{10}$ EID_{50}/mL with SD. (D) Wild-type and mutant viruses (10 μl) were deposited onto 96-well plates and were incubated in an environmental chamber set for 20 °C, 50% relative humidity for the indicated lengths of time. Six replicates for each time point were collected by reconstitution in 60 μl of PBS and viral titers were determined in eggs and are expressed as the mean $\log_{10}$ EID_{50}/mL with SD. Limit of detection (< 1 $\log_2$ HA units or 1.5 $\log_{10}$ EID_{50}/ml) is indicated by dashed lines. Two-way analysis of variance followed by Sidak's multiple comparisons test between the wild-type and the mutant virus was performed with GraphPad Prism. *, $p \leq 0.05$; **, $p \leq 0.01$; ‡, $p \leq 0.0001$.

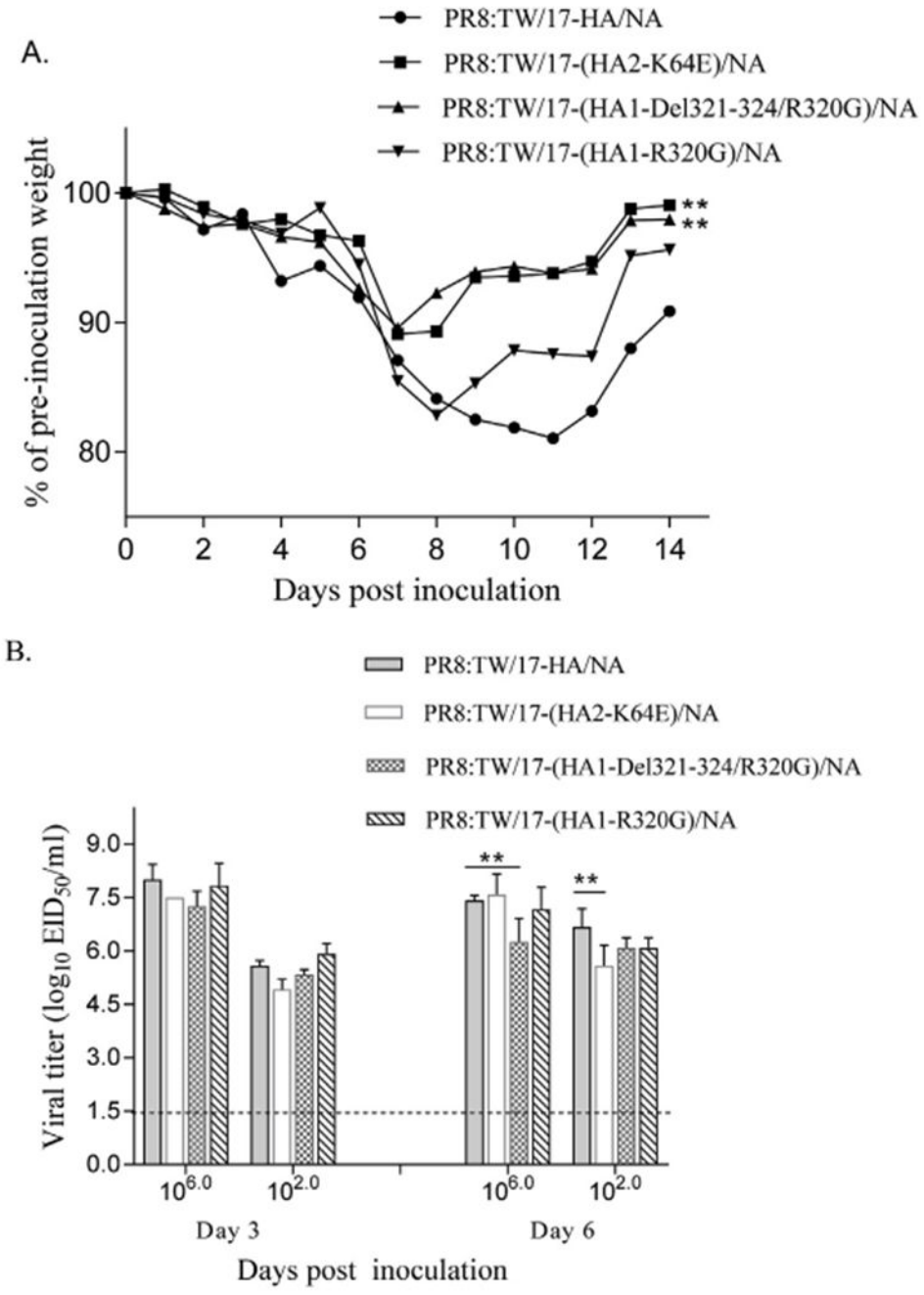

Fig. 7. Replication of recombinant PR8:TW/17-HA/NA viruses in mice.

(A) Groups of five mice each were intranasally inoculated with $10^{3.0}$ EID_{50} of the recombinant PR8 viruses expressing wild-type or mutant TW/17 virus HAs and were monitored for morbidity and mortality for 14 days. The graph represents the mean percentages of pre-inoculation weight. The difference between weight loss of wild-type and each of the mutant virus groups was analyzed by one-way ANOVA based on calculated Area Under the Curve (AUC) with GraphPad Prism. (B) Groups of three mice each were intranasally inoculated with $10^{6.0}$ or $10^{2.0}$ EID_{50} of wild-type or mutant virus. Lung tissues

collected on day 3 or 6 p. i. were titrated in eggs and viral titers were plotted as the mean with SD. Statistical analyses were performed using two-way analysis of variance with GraphPad Prism. **, $p < 0.01$.